NANO LETTERS

Letter

pubs.acs.org/NanoLett

Cell−Substrate Dynamics of the Epithelial-to-Mesenchymal Transition

Thilo Baronsky,[†] Daja Ruhlandt,[‡] Bastian Rouven Brückner,[†] Jonas Schäfer,[§] Narain Karedla,[‡] Sebastian Isbaner,[‡] Dirk Hähnel,[‡] Ingo Gregor,[‡] Jörg Enderlein,[‡] Andreas Janshoff,*[,†] and Alexey I. Chizhik*[,‡]

[†]Institute of Physical Chemistry, University of Göttingen, Tammannstr. 6, 37077 Göttingen, Germany

[‡]Third Institute of Physics, University of Göttingen, Friedrich-Hund-Platz 1, 37077 Göttingen, Germany

[§]Institute of Organic and Biomolecular Chemistry, University of Göttingen, Tammannstr. 2, 37077 Göttingen, Germany

Supporting Information

ABSTRACT: The biological process of the epithelial-to-mesenchymal transition (EMT) allows epithelial cells to enhance their migratory and invasive behavior and plays a key role in embryogenesis, fibrosis, wound healing, and metastasis. Among the multiple biochemical changes from an epithelial to a mesenchymal phenotype, the alteration of cellular dynamics in cell−cell as well as cell−substrate contacts is crucial. To determine these variations over the whole time scale of the EMT, we measure the cell−substrate distance of epithelial NMuMG cells during EMT using our newly established metal-induced energy transfer (MIET) microscopy, which allows one to achieve nanometer axial resolution. We show that, in the very first hours of the transition, the cell−substrate distance increases substantially, but later in the process after reaching the mesenchymal state, this distance is reduced again to the level of untreated cells. These findings relate to a change in the number of adhesion points and will help to better understand remodeling processes associated with wound healing, embryonic development, cancer progression, or tissue regeneration.

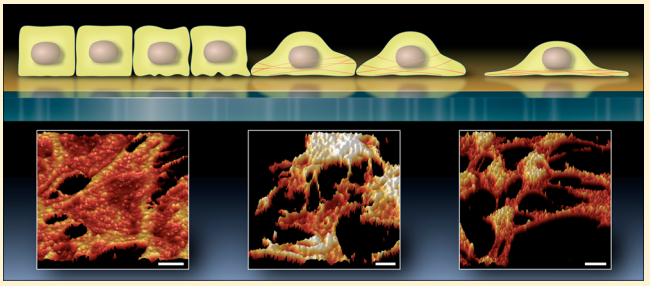

KEYWORDS: *Cell−substrate distance, integrin, MIET microscopy, plasmonics, super-resolution microscopy, EMT*

The process that epithelial cells can change into mesenchymal cells, either fully or only partially, is referred to as the epithelial to mesenchymal transition (EMT). EMT occurs in many biological processes, such as embryogenesis, tissue regeneration, and wound healing, as well as in fibrosis or cancer progression.[1−3] The transition is characterized by a switch of the cellular phenotype comprising loss of cell junctions, apical−basal polarity, reorganization of the cytoskeleton, change of cell shape, mechanical properties such as cortical tension, and gene expression.[1,2,4−6] Well-known stimulating agents for the transition from a highly structured and polarized epithelial cell layer with strong cell−cell contacts to single mesenchymal cells are specific growth factors like those from the transforming growth factor-β (TGF-β) superfamily.[1] The transcriptional program for EMT induced by TGF-β is known to be coordinated primarily through Smad-dependent activation of transcription factors of the Snail, ZEB, and Twist families.[7] Interestingly, it has been reported that the cytokine TGF-β has a suppressing influence on malignant cells at early tumor stages, whereas later it fosters metastasis through EMT.[8] Mesenchymal cells display an elongated morphology with a front-rear polarization and a strong adhesion to the extracellular matrix via focal contacts and focal adhesions. The ability of mesenchymal cells to remodel their surrounding extracellular matrix is a key determinant for tumor dissemination. The tumor suppressing effects are in contrast to tumor promoting effects such as extracellular matrix (ECM) remodeling and increased invasiveness, which has led to a large number of studies targeting the impact of TGF-β on different cell lines.[2,5,9] However, it was found that an induced EMT is rarely observed in vitro. The mouse mammary gland epithelial cell line NMuMG and the proximal tubular epithelial cell line MCT undergo EMT in response to TGF-β1 exposure.[10,11] Other cell lines such as HMECs and HEKs show a spindle shape and form actin stress fibers in response to TGF-β1 treatment but maintain their adherens junctions. HaCat or Colo357 cells only form stress fibers when treated with the growth factor for 48 h.[11] Apart from cytokines, the cell's microenvironment including adjacent cells, curvature, elasticity, and the extracellular matrix might also have an impact on tumor progression.[12] The characteristic changes during EMT, including structural and invasive properties, are mediated by signaling cascades, which can be subdivided into Smad and non-Smad pathways.[1] Transforming growth factor-β signals

Received: April 13, 2017
Revised: April 24, 2017
Published: April 25, 2017

DOI: 10.1021/acs.nanolett.7b01558
Nano Lett. 2017, 17, 3320−3326

through a tetrameric complex of type I and type II receptors, which activate Smad2 and Smad3 that are eventually combined with Smad4.[1] This Smad complex translocates into the nucleus and together with transcription regulators affects gene regulation, finally resulting in actin reorganization as well as alterations in cell−cell and cell−substrate interactions.

The difference between an epithelial versus a mesenchymal state is not very distinct, and also partial EMTs are observed. This range of morphological changes demonstrates the enormous flexibility of assumedly differentiated cells during morphogenesis.[13] Among the switch in morphology, the modification of the cell−substrate and cell−cell interaction is one of the hallmarks of the EMT.[7,14,15] It was recently shown that also mechanical properties of NMuMG cells are considerably altered to accommodate the challenges associated with an increase in cell surface area due to the switch in morphology.[16−18] Cortical tension as well as membrane tension is gradually increased during EMT until values close to that of fibroblasts or individual cells are reached.[19] Employing cell−substrate impedance sensing, Schneider et al. found that, upon triggering of the EMT in confluent NMuMG cells using the cytokine TGF-β1, the cells show a temporal increase in micromotion, i.e., an increase in cell−substrate dynamics lasting 4−9 h.[20] This state—referred to as the *transitional state I*—characterized by vivid cell−substrate dynamics is only transient and superseded by the so-called *transitional state II*, where the cellular adhesion is proposed to increase and suppresses the fluctuations.[20] The complete loss of cell−cell contacts followed by a switch of the phenotype characterize this state. However, a precise picture of the process on a cellular or even subcellular level is lacking due to limited spatial resolution especially in the *z*-direction.

Here, we investigated the response of NMuMG cells to administration of TGF-β1 at different stages of the EMT starting from the initial disassembly of cell−cell contacts to the final reorganization of cytoskeleton representing the mesenchymal phenotype. Because the cell−substrate distance as inferred from impedance measurements seems to be affected (especially in the early stages of the transition), we deployed the recently developed metal-induced energy transfer (MIET) microscopy, which allowed us to measure the axial localization of the basal cell membrane with 2−3 nm accuracy.[21]

The principle of MIET imaging is based on the energy transfer between a fluorescent molecule and a metal surface, which results in the molecule's de-excitation rate acceleration and can be observed as a shortening of its fluorescence lifetime.[21,22] Because the energy transfer rate is monotonically dependent on the distance of a molecule from the metal layer within the first 200 nm, the fluorescence lifetime can be directly converted into a distance between the emitter and metal surface within this range of distances. Figure 1 shows the setup used in this study to measure the cell−substrate distance, referred to as *height*.

First we studied whether we could reproduce the hallmarks of EMT to ensure a proper response of cultured NMuMG cells to the administration of the cytokine TGF-β1.[10,23] One hallmark of EMT is the downregulation of E-cadherin to initiate destabilization of adherens junctions. In turn, the downregulation of E-cadherin is counterbalanced by the increased expression of mesenchymal neural cadherin (N-cadherin) leading to an altered cell adhesion. Supplementary Figure S1 confirms the cadherin switch showing Western blots of E-cadherin and N-cadherin expression after the administration of TGF-β1 for 48 h.[10,23] Additionally, the EMT requires repression of genes encoding for proteins participating in formation of tight junctions.[1] In previous studies we used electric cell−substrate impedance sensing to show how cell−cell contacts, i.e., tight junctions become leaky. Altogether these changes in protein expression prevent the de novo formation of epithelial cell−cell junctions and result in the loss of the epithelial barrier function.[1] Figure 2 illustrates the morphological changes of NMuMG cells in response to cytokine TGF-β1 exposure using phase contrast microscopy, fluorescence microscopy (confocal laser scanning microscopy), and MIET microscopy. The phase contrast images in Figure 2a and b show how the general phenotype of NMuMG cells transformed from an ordered polarized epithelial cell layer to individual, elongated mesenchymal-like cells. After 48 h of TGF-β1 treatment, the NMuMG cells occupy a larger area compared to untreated cells. The fluorescence images reveal that the F-actin (red) is reorganized to well-defined stress fibers, which traverse the entire cell (Figure 2c and d). This remodeling of the F-actin network is typical for these cells passing through the EMT.[10,24] Immunostaining of E-cadherin confirms the reduction of E-cadherin expression in the cells after exposure to TGF-β1 (Figure 2e and f). It was found that after 48 h of TGF-β1 treatment the amount of E-cadherin is significantly reduced (Supplementary Figure S1). The observed modifications in the cellular structure after administration of TGF-β1 clearly confirm that induction of the EMT in our cells was successful.

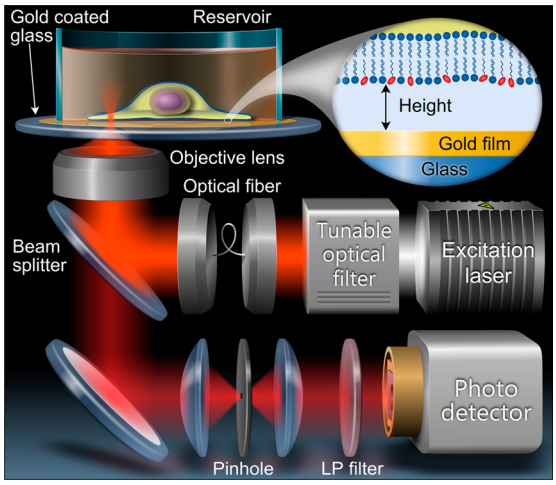

Figure 1. Scheme of the experimental setup for MIET microscopy (LP: long pass).

For MIET measurements we used a semitransparent 20 nm gold film deposited on a glass cover slide. To map the distance between the cell and the surface, we stained the cellular plasma membrane with a fluorophore (CellMask Deep Red) and measured their fluorescence lifetime to obtain the fluorophore−metal distance (see Supplementary Table S1 for the number of used cells). Figure 2g−h and i−j shows the fluorescence intensity and lifetime images of the basal membrane of NMuMG cells. We used the lifetime information for reconstructing a three-dimensional map of the basal membrane shown in Figure 2k−l as reported previously.[21] Figure 2k shows untreated NMuMG cells in a partially confluent monolayer. The confocal *z*-stack shown in Supplementary Figure S2 confirms that indeed only the basal membrane is captured to generate MIET images. Figure 2l depicts a cluster of transformed cells after treatment with TGF-β1 for 48 h. The

DOI: 10.1021/acs.nanolett.7b01558
Nano Lett. 2017, 17, 3320−3326

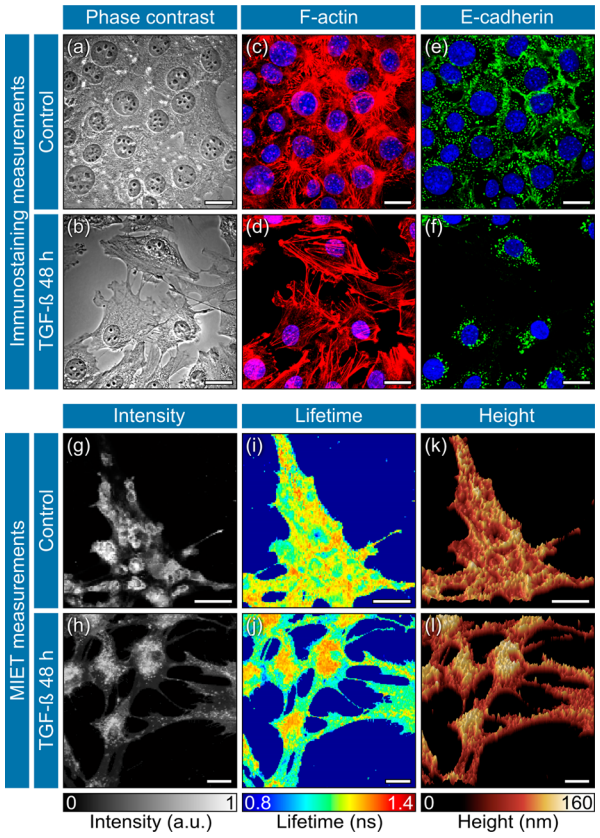

Figure 2. NMuMG cells without (a, c, e, g, i, k) and after exposure to TGF-β1 (10 ng/mL) for 48 h (b, d, f, h, j, l). Top panel: TGF-β1 induced shape changes of NMuMG cells. (a, b) Phase contrast images. (c, d) Confocal fluorescence microscopy images of the F-actin cytoskeleton (red, Alexa Fluor 546–phalloidin) and nuclei (blue, DAPI). (e, f) Confocal fluorescence microscopy images of fluorescently marked E-cadherin (green, Alexa Fluor 488) and nuclei (blue, DAPI). Bottom panel: Fluorescence lifetime imaging and three-dimensional reconstruction of the basal cell membrane in response to TGF-β1 treatment. (g, h, i, j) Simultaneously acquired fluorescence intensity (g, h) and lifetime (i, j) images of the basal membrane of living NMuMG cells grown on a gold-covered glass substrate. (k, l) Three-dimensional profiles computed from fluorescence lifetime images. Each row of images shows the same cells. Scale bars: 20 μm.

images clearly show that NMuMG cells undergo morphological transformations from a compact epithelial type toward a more fusiformic mesenchymal shape in response to TGF-β1 treatment and that it is possible to spatially resolve the distance between the basal membrane of the cell and the gold substrate using MIET microscopy. Since z-resolution of MIET microscopy is in the nanometer regime, it was possible to address also changes of the cell–substrate distance with unprecedented spatial resolution. It was suggested by micromotion measurements using electric cell–substrate impedance sensing that the early dynamics of the cell–substrate distance after TGF-β1 administration is potentially interesting and complex. ECIS, however, allows only to collect data from a number of cells simultaneously and therefore lacks spatial information.[20]

In Figure 3a, time-elapsed MIET images of NMuMG cells during the EMT are used to monitor height changes, i.e., changes of the cell–substrate distance as a function of time, during TGF-β1 treatment. The time interval (0–48 h) was chosen in a way that it covers all relevant stages of transformation as depicted in the cartoon above. Especially, transitional state I was of interest since cell–substrate variations were found to be highest during this regime, maybe the earliest detectable response to TGF-β1 administration. The corresponding, reconstructed three-dimensional structures of the basal membrane are shown in the central panel of Figure 3. Images were recorded 0 h (b), 12 h (c), 24 h (d), 48 h (e), and 72 h (f) after treatment with TGF-β1 (see Supplementary Figure S3 for how picture analysis is carried out from fluorescence lifetime images). In response to cytokine administration the NMuMG cells change their phenotype from an epithelial ordered cell layer (b) to separated cells with increasing cell size (e, f). At the end of the process mesenchymal cells exhibit a more homogeneous distance between the basal membrane and the surface (e, f) compared to cells at the beginning of the EMT (b, c). Interestingly, this was also found comparing the cell–substrate distance of MDCK II cells with that of malignant MDA-MB231 cells.[21] The mesenchymal cancer cell line MDA-MB231 displays a rather smooth basal membrane, i.e., a rather constant distance from the surface, whereas epithelial MDCK II cells display a rather wavy structure of the height between basal membrane and substrate. Some points/areas are very close to the surface. We refer to them as *adhesion points* throughout the text since the precise molecular nature of the contacts is not clear (vide infra).

In Figure 3a every red solid circle represents the average height between the basal cell membrane and the substrate collected from randomly picked cells at different time points during cytokine treatment as indicated. For each time point the average fluorescence lifetime of around 10–30 cells was calculated. The corresponding histograms of all cells taken at five prominent time points after TGF-β1 addition are shown in Figure 3g–k exemplarily [0 h (g), 12 h (h), 24 h (i), 48 h (j), and 72 h (k)]. The colored error band indicates the standard error of the mean of the height values obtained at the corresponding time point. Untreated cells maintain a constant average cell membrane–substrate distance of approximately 110–120 nm during the whole observation time (blue dots). After incubation with TGF-β1, cells respond by increasing the basal membrane–substrate distance from around 120 nm up to 156 nm. After reaching the maximal distance of 156 nm around 5 h after initiation of the EMT by addition of TGF-β1, the cell–substrate distance decreases again within the following 14 h until reaching the average level of untreated cells again. After 48 h of TGF-β1 treatment the NMuMG cells maintain the same average cell–substrate distance as untreated cells over the same period of time. Cells were measured up to 72 h without noticeable change of the average distance (data not shown). Comparison with the cell–substrate distance measured for the untreated cells (Figure 3, blue curve) reveals that cells change their distance to the substrate transiently only in response to TGF-β1 treatment. Note that the distance from the surface and not from the extracellular matrix with its finite thickness is reported. It is conceivable that secretion of extracellular matrix proteins is responsible for this effect. This is, however, not very likely to be the sole explanation since adhesion points display the same distance between cell membrane and substrate regardless of the time period of TGF-β1 exposure. In contrast, the number of these adhesion points decreases, and the height in between adhesion points rises (vide infra).

Not only actin reorganization and dissolution of cell–cell junctions but also remodeling of focal adhesions accompanies the transition from the epithelial phenotype to the mesen-

DOI: 10.1021/acs.nanolett.7b01558
Nano Lett. 2017, 17, 3320–3326

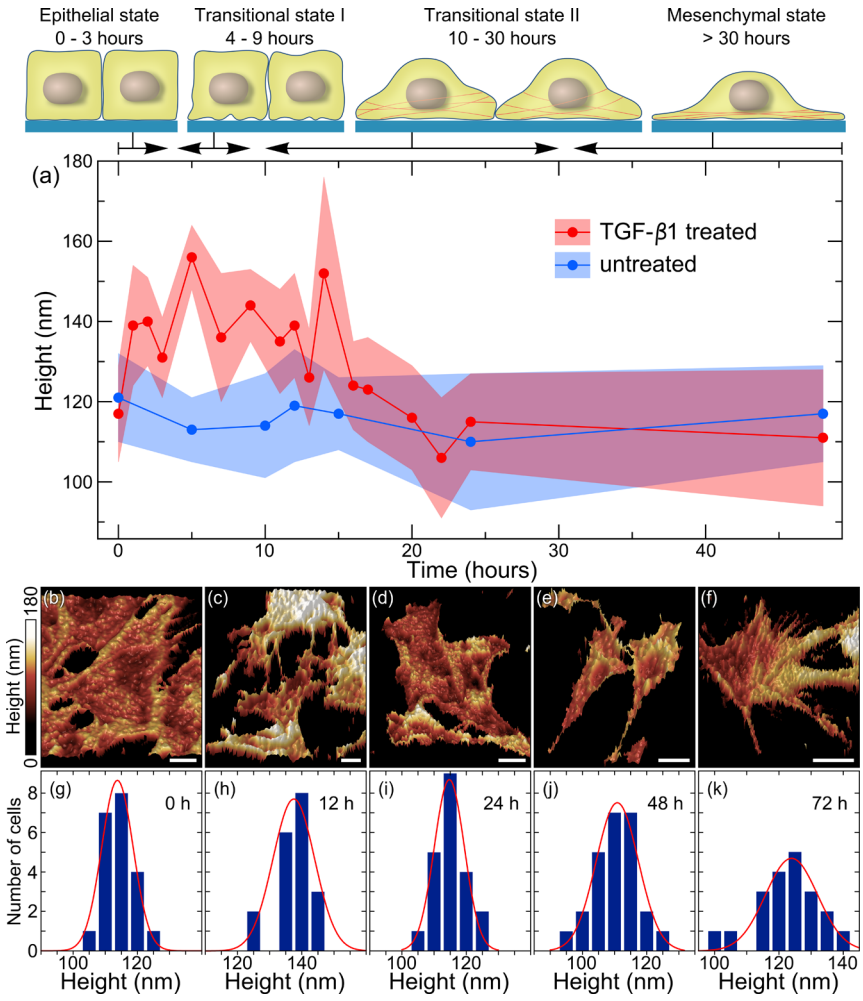

Figure 3. (a) Average cell membrane-substrate distance of untreated (blue) and TGF-β1 treated NMuMG cells (red) over time. NMuMG cells detach from the surface by more than 20 nm on average in response to TGF-β1 administration. After 20 h the initial cell−substrate distance is restored. The standard error of mean (SEM) is illustrated as colored area around the data points. (b−f) Three-dimensional reconstruction of the basal cell membrane at different stages of EMT. Three-dimensional height profiles computed from fluorescence lifetime images of NMuMG cells recorded after 0 h (b), 12 h (c), 24 h (d), 48 h (e), and 72 h (f) of TGF-β1 treatment (10 ng/mL); scale bars: 20 μm. (g−k) Histograms showing the distribution of all height profiles at one distinct time point as indicated.

chymal state. Binding of TGF-β1 to type I receptors leads to phosphorylation of these receptors. Smad2/3 is activated, translocates together with Smad4 into the nucleus and acts as transcription factor. Cellular adhesion molecules are activated via a Rac/Cdc42 pathway.[25] Therefore, we followed the motion of TGF-β1 treated NMuMG cells over the surface with an axial resolution of 2−3 nm for 6 h to monitor the dynamics of the adhesion points (Figure 4). This time period comprises the initial and strongest changes in cell−substrate distances. Control cells kept under identical conditions neither show an increase in the distance nor a decrease at later time. To avoid that loss of cell vitality during imaging interferes with our results, we took different cells (color coded). Each color represents the cell−substrate distance obtained from lifetime imaging of a single cell analyzed for approximately 1.5 h. For some samples we were able to investigate two cells simultaneously, reflected in an overlay of two data sets. Control cells not treated with the cytokine (continuous and dotted black lines) were only considered in the two relevant time periods where obvious changes in cell−substrate distance occurred due to TGF-β1 administration. One fluorescence intensity image was taken every 2 min to monitor the beginning of EMT with high time resolution and only moderate photo bleaching of the dye. This temporal resolution would in principle be in line with the expected turn over time of focal adhesions.[26] In the first hour after inducing EMT the cells lift up from the surface as expected from our averaged data shown in Figure 3. The cell−substrate distance increases from approximately 110 to 145 nm and stays at this level for the next 5 h with large fluctuations. Afterward the cell−substrate distance (height) decreases again to the level of untreated cells. Figure 4b and the insets of Figure 4a show MIET snapshots of cells incubated with TGF-β1 obtained at different time points after administration of the cytokine. These reconstructed three-dimensional images of the basal membrane illustrate the dynamics of NMuMG cells lifting up from the surface after initiating the EMT. The 3D membrane profiles shown in Figure 4b illustrate how the cell detaches from the surface, while largely keeping the position of the adhesion points. Interestingly, both the number of regions where the cell membrane is in close contact to the substrate decreases as well as the distance of the basal cell membrane between the adhesion points increases, leading to an overall increase of the average cell−substrate distance. This is best illustrated by the

DOI: 10.1021/acs.nanolett.7b01558
Nano Lett. 2017, 17, 3320−3326

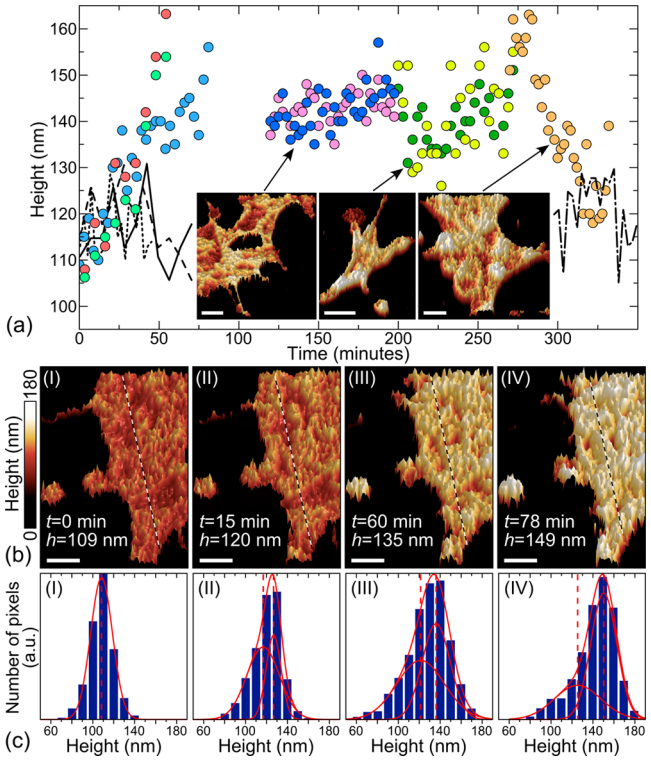

Figure 4. Time-elapsed imaging of the cell−substrate distance. (a) Cell−substrate distance of NMuMG cells exposed to TGF-β1 (10 ng/mL) monitored over the first 6 h after addition of the cytokine. Each color represents the time-dependent change of the cell−substrate distance (height) of an individual cell. 0−80 min (red, light green, light blue), 120−200 min (dark blue, purple), 200−270 min (dark green, yellow), 270−330 min (orange). Inset: Representative three-dimensional profiles, computed from fluorescence lifetime images of NMuMG cells of each measurement at time points as indicated (120−200 min, 200−270 min, 270−330 min). (b) Three-dimensional reconstruction of the basal cell membrane, computed from fluorescence lifetime images of a single NMuMG cell at four different time points (I−IV) as indicated. The height scale applies to all images shown in panels a and b. Scale bars: 20 μm. The profiles along the dashed black and white lines are shown in Figure 5a. (c) Histograms showing the pixel height distribution of the basal membrane depicted in panel b. Red solid curves show the fit to the experimental data with Gaussian functions. Red dashed vertical lines show maxima of the Gaussian distributions.

corresponding histograms (Figure 4c), where a clear skewness of the distribution toward larger height values becomes visible after administration of TGF-β1. We therefore decomposed the histograms into two populations for $t > 0$ h by fitting two Gaussian distributions to the data (red lines). We attribute the distribution centered around lower distances to adhesion points and the one centered around higher values to the cell membrane in between these adhesion points. We found that within 78 min both populations clearly separate and the amount of membrane not associated with adhesion points rises substantially (see Supplementary Table S2). In particular, the generally larger values corresponding to the cell membrane in between the adhesion points move toward higher values (from approximately 110 to 150 nm) over time. In contrast, the lower values, i.e., the distance values representing the adhesion points, increase only from 110 to 120 nm in the same time interval (78 min), which might be attributed to the production of extracellular matrix proteins. Control experiments with untreated cells show a constant average cell−substrate distance of around 110−125 nm for the entire measuring time (see also Figure 3). This confirms that the changes in the time series of TGF-β1 treated NMuMG cells are caused by the onset EMT and do not originate from the measurement itself.

Figure 5 shows four consecutively acquired cross sections (stacked) of the cell membrane−metal surface distance recorded within the first 1.5 h of the EMT. Dissolution (black arrowheads) and formation (red arrowheads) of adhesion points are indicated. On average more adhesion sites are lost than newly formed during this time period, and the distance of the membrane in between also increases as discussed above. The process reverses after 250 min of TGF-β1 treatment. During the EMT the molecular expression pattern changes dramatically. Most prominently, the level of E-cadherin, which is the major component of adherens junctions, is reduced, and N-cadherin is expressed instead. Since E-cadherin-mediated adherens junctions are anchored to the actin cytoskeleton via their cytoplasmic domains, the dissolution of cell−cell junctions changes the organization of the actin cytoskeleton from a cortex-dominating one to one where contractile stress fibers prevail. Increased motility is generally facilitated by reduced adhesion explaining the general trend in the early stages of EMT, where we found an increase in cell−substrate distance together with an increased micromotion.[20]

Generally, the smallest distance between the basal membrane and the metal surface was found to be 40−60 nm. We attribute this minimal height to the site where persistent molecular interactions occur. Considering the thickness of the ECM and possible cell adhesion molecules, this is reasonable. Although we could not assign adhesion points found in MIET microscopy to focal adhesions unequivocally, we found a similar pattern of integrins (immunostaining of β1 chain) distributed in the basal cell membrane (Figure 5b−e). Notably, however, we did not find a significant difference in the pattern of integrins before and after cytokine addition (80 min after TGF-β1 addition) suggesting that MIET microscopy might actually capture other processes as well. On longer time scales (48 h), however, an increase in the expression level of integrin β1 is found (Supplementary Figure S1). We propose that cells detach and lift-off from the surface because the expression pattern for cell adhesion molecules changes. Even if we cannot explicitly correlate our observation with the temporal expression pattern of specific proteins, it is conceivable that for instance the reorganization of focal contacts during EMT contributes to the temporal change in cell−substrate distance. Surprisingly, mesenchymal cells exhibit a smoother interface, i.e., a more homogeneous spatial cell−substrate distance distribution compared to polarized epithelial cells, which might be due to presence of stress fibers and the elevated tension of the mesenchymal phenotype.

Interestingly, the time period in which the cells are further apart from the surface corresponds roughly to the time the transepithelial resistance of a confluent NMuMG monolayer drops upon TGF-β1 treatment and relates to the so-called transitional state I (early after TGF-β1 exposure) and transitional state II (10−30 h after TGF-β1 addition).[20] Detrended fluctuation analysis of micromotion revealed that not only the variance increases but also the Hurst coefficient, which reports on long-term memory in time series data, increased substantially during this time indicative of active processes generating long memory fluctuations also explainable by the lift-off process found in this study.[27] During transitional

DOI: 10.1021/acs.nanolett.7b01558
Nano Lett. 2017, 17, 3320−3326

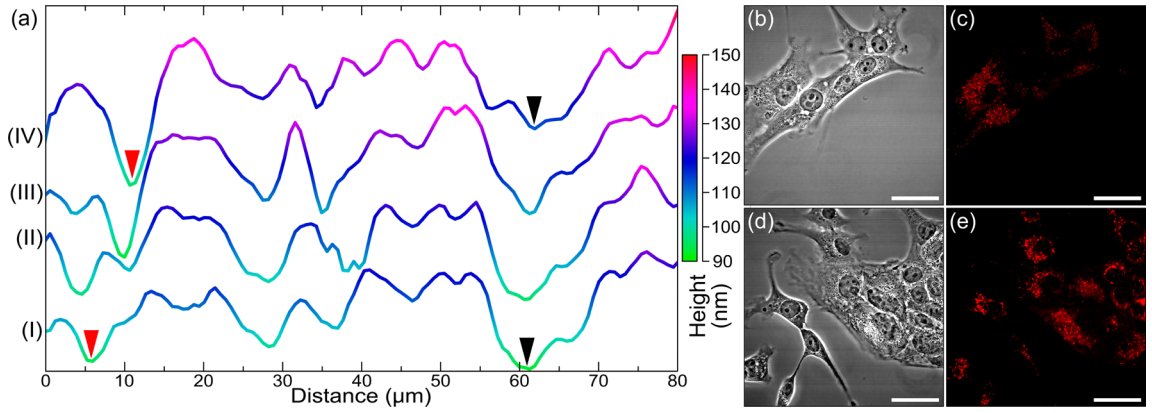

Figure 5. (a) Time-dependent height profiles of the basal cell membrane of NMuMG cells. Cross sections were taken in dependence of the distance to the metal surface at different time points (0−80 min) after addition of TGF-β1 (dashed lines in Figure 4b). Red arrows indicate the formation of a new focal adhesion point, while black ones indicate the dissolution of a focal adhesion site. (b−e) Integrin β1 distribution in NMuMG cells. (b, d) Phase contrast images of untreated (b) and TGF-β1 treated cells for 80 min (d), respectively. (c, e) Confocal fluorescence images of integrin β1 of untreated cells (c) and cells exposed to TGF-β1 for 80 min (e), respectively. The focus was set to the basal cell side. Scale bars: 30 μm.

states I and II, we found that cortical tension and membrane tension increase only slightly, leading to the conclusion that in these initial states removal of cell−cell contacts prevails over reorganization of the cytoskeleton, leading to a different mechanical phenotype.[19]

After completion of this initial process, the original distance between cell and substrate is restored. This phenomenologically correlates with recent findings that β5-integrins are required for TGF-β1 induced EMT anchoring the cells at specific matrix sites and thereby mediate cell stretching that eventually leads to disruption of cell−cell contacts.[28] The interplay of cytoskeleton reorganization and the dynamic removal and formation of new adhesion sites has been predicted but never been shown in a direct manner. Monitoring the EMT-induced modulation of the cell−substrate distance requires nanometer axial resolution over a height variation of the basal membrane of nearly 200 nm. The axial resolution of MIET microscopy exceeds those of the existing super-resolution techniques by 1 order of magnitude, while the range of the measurable dye−substrate distances fully covers the expected modulation of the basal membrane height. As a result, MIET microscopy bridges the realm of FRET[29,30] imaging and super-resolution methods,[31−35] being a powerful tool for monitoring cellular adhesion with unprecedented axial resolution.

In conclusion, we propose that epithelial cells subject to cytokine TGF-β1 treatment respond by a complex pattern of dynamic remodeling of adhesion sites, which enables the cells to lift-off from the surface entering a stage of increased vertical motility. We found that this state is transient and mesenchymal cells eventually become quiescent again, assuming higher adhesion forces as inferred from the smaller cell−substrate distance. The obtained results shine light on the highly dynamic initial stages of the EMT prior to cytoskeleton remodeling allowing the cell to become mobile and to occupy a larger area. The EMT causes an architectural and morphological remodeling of the local environment at the surface of the transitioning cell. This coordinate action enforces an alteration of most of the intercellular adhesion complexes such as adherent junctions and tight junctions allowing for complete detachment of cells from their neighbors. These changes, together with the de novo synthesis of adhesion molecules and ECM components, enable the transitioned cells to migrate. It is conceivable that the initial phase after TGF-β1 administration, during which the cells lift-off from the substrate, is the decisive step, where the reprogramming of the phenotype starts.

■ ASSOCIATED CONTENT

Supporting Information

The Supporting Information is available free of charge on the ACS Publications website at DOI: 10.1021/acs.nanolett.7b01558.

More detailed information regarding the experimental methods including MIET imaging setup, fluorescence lifetime data evaluation, cell culture, plasma membrane staining, fluorescence microscopy, Western blotting, and the supplementary figures and tables (PDF)

■ AUTHOR INFORMATION

Corresponding Authors

*A.J.: E-mail: ajansho@gwdg.de, Phone: +49-551-3910633.
*A.I.C.: E-mail: alexey.chizhik@phys.uni-goettingen.de, Phone: +49-551-397723.

ORCID

Alexey I. Chizhik: 0000-0003-0454-5924

Author Contributions

T.B., D.R., and B.R.B. contributed equally to this work.

Notes

The authors declare no competing financial interest.

■ ACKNOWLEDGMENTS

Funding granted by the German Science Foundation [SFB 937 (projects A05 and A14), SPP 1782 (AJ), SFB 803 (project A07), SFB 860 (project A6), and CNMBP] is gratefully acknowledged.

■ REFERENCES

(1) Lamouille, S.; Xu, J.; Derynck, R. *Nat. Rev. Mol. Cell Biol.* **2014**, *15*, 178.
(2) Kalluri, R.; Weinberg, R. A. *J. Clin. Invest.* **2009**, *119*, 1420.
(3) Son, H.; Moon, A. *Toxicol. Res.* **2010**, *26*, 245.
(4) Kalluri, R. *J. Clin. Invest.* **2009**, *119*, 1417.
(5) Thiery, J. P.; Acloque, H.; Huang, R. Y.; Nieto, M. A. *Cell* **2009**, *139*, 871.
(6) Thiery, J. P.; Sleeman, J. P. *Nat. Rev. Mol. Cell Biol.* **2006**, *7*, 131.
(7) Xu, J.; Lamouille, S.; Derynck, R. *Cell Res.* **2009**, *19*, 156.

DOI: 10.1021/acs.nanolett.7b01558
Nano Lett. 2017, 17, 3320−3326

(8) Pardali, K.; Moustakas, A. *Biochim. Biophys. Acta, Rev. Cancer* **2007**, *1775*, 21.
(9) Chapman, H. A. *Annu. Rev. Physiol.* **2011**, *73*, 413.
(10) Haynes, J.; Srivastava, J.; Madson, N.; Wittmann, T.; Barber, D. L. *Mol. Biol. Cell* **2011**, *22*, 4750.
(11) Brown, K. A.; Aakre, M. E.; Gorska, A. E.; Price, J. O.; Eltom, S. E.; Pietenpol, J. A.; Moses, H. L. *Breast Cancer Res.* **2004**, *6*, R215.
(12) Gao, D.; Vahdat, L. T.; Wong, S.; Chang, J. C.; Mittal, V. *Cancer Res.* **2012**, *72*, 4883.
(13) Tsai, J. H.; Yang, J. *Genes Dev.* **2013**, *27*, 2192.
(14) Xie, L.; Law, B. K.; Aakre, M. E.; Edgerton, M.; Shyr, Y.; Bhowmick, N. A.; Moses, H. L. *Breast Cancer Res.* **2003**, *5*, R187.
(15) Zhang, J.; Tian, X. J.; Zhang, H.; Teng, Y.; Li, R.; Bai, F.; Elankumaran, S.; Xing, J. *Sci. Signaling* **2014**, *7*, ra91.
(16) Gal, A.; Sjoblom, T.; Fedorova, L.; Imreh, S.; Beug, H.; Moustakas, A. *Oncogene* **2008**, *27*, 1218.
(17) Shirakihara, T.; Saitoh, M.; Miyazono, K. *Mol. Biol. Cell* **2007**, *18*, 3533.
(18) Netherton, S. J.; Bonni, S. *PLoS One* **2010**, *5*, e13971.
(19) Schneider, D.; Baronsky, T.; Pietuch, A.; Rother, J.; Oelkers, M.; Fichtner, D.; Wedlich, D.; Janshoff, A. *PLoS One* **2013**, *8*, e80068.
(20) Schneider, D.; Tarantola, M.; Janshoff, A. *Biochim. Biophys. Acta, Mol. Cell Res.* **2011**, *1813*, 2099.
(21) Chizhik, A. I.; Rother, J.; Gregor, I.; Janshoff, A.; Enderlein, J. *Nat. Photonics* **2014**, *8*, 124.
(22) Karedla, N.; Chizhik, A. I.; Gregor, I.; Chizhik, A. M.; Schulz, O.; Enderlein, J. *ChemPhysChem* **2014**, *15*, 705.
(23) Avery-Cooper, G.; Doerr, M.; Gilbert, R. W.; Youssef, M.; Richard, A.; Huether, P.; Viloria-Petit, A. M. *Cancer Cell Int.* **2014**, *14*, 19.
(24) Shankar, J.; Nabi, I. R. *PLoS One* **2015**, *10*, e0119954.
(25) Edlund, S.; Landstrom, M.; Heldin, C. H.; Aspenstrom, P. *Mol. Biol. Cell* **2002**, *13*, 902.
(26) Kaverina, I.; Krylyshkina, O.; Small, J. V. *Int. J. Biochem. Cell Biol.* **2002**, *34*, 746.
(27) Schneider, D.; Janshoff, A. *Biochem. Biophys. Res. Commun.* **2012**, *419*, 221.
(28) Bianchi, A.; Gervasi, M. E.; Bakin, A. *Cell Cycle* **2010**, *9*, 1647.
(29) Wu, P.; Brand, L. *Anal. Biochem.* **1994**, *218*, 1.
(30) Clegg, R. M. *Curr. Opin. Biotechnol.* **1995**, *6*, 103.
(31) Hell, S. W. *Nat. Biotechnol.* **2003**, *21*, 1347.
(32) Hell, S. W. *Nat. Methods* **2009**, *6*, 24.
(33) Chizhik, A. M.; Stein, S.; Dekaliuk, M. O.; Battle, C.; Li, W.; Huss, A.; Platen, M.; Schaap, I. A. T.; Gregor, I.; Demchenko, A. P.; Schmidt, C. F.; Enderlein, J.; Chizhik, A. I. *Nano Lett.* **2016**, *16*, 237.
(34) Rust, M. J.; Bates, M.; Zhuang, X. W. *Nat. Methods* **2006**, *3*, 793.
(35) Betzig, E.; Patterson, G. H.; Sougrat, R.; Lindwasser, O. W.; Olenych, S.; Bonifacino, J. S.; Davidson, M. W.; Lippincott-Schwartz, J.; Hess, H. F. *Science* **2006**, *313*, 1642.

DOI: 10.1021/acs.nanolett.7b01558
Nano Lett. 2017, 17, 3320−3326